



Cite this: *Soft Matter*, 2025,
21, 427

Magnetic microwire rheometer reveals differences in hydrogel degradation *via* disulfide reducing agents[†]

Margaret Braunreuther,^{ID a} Justin Arenhoevel,^b Raju Bej,^b Cody Moose,^c Marcus A. Mall,^{def} Rainer Haag^{*b} and Gerald G. Fuller^{ID *a}

Mucus is composed of a complex network of mucin polymers connected by disulfide bonds. In muco-obstructive diseases, an increase in mucin disulfide crosslinks contributes to pathologic mucus formation, characterized by an increase in mucus viscosity and stiffness. Reducing agents that break down the disulfide bonds between mucins can be used to treat pathologic mucus and restore healthy mucus flow properties. Here, we compare three reducing agents *via* a rheological assay. A mucus-mimetic disulfide-crosslinked hyaluronic acid hydrogel was treated with thiolated dendritic polyglycerol sulfate (dPGS-SH), *N*-acetylcysteine (NAC), or dithiothreitol (DTT). A magnetic microwire rheometer was used to track the rheology of the hydrogel over time as the treatment degraded the sample. This nondestructive and minimally invasive technique reveals differences in the degradation mechanism between these reducing agents, with potential implications for drug delivery and the treatment of muco-obstructive diseases.

Received 21st September 2024,
Accepted 7th December 2024

DOI: 10.1039/d4sm01118j

rsc.li/soft-matter-journal

Introduction

Mucus is a biological hydrogel composed of a network of polymeric mucins. The biophysical properties of mucus are determined by the structure of this network, which is mediated by a variety of factors, such as the concentration of mucins and the density of covalent and physical interactions.^{1–3} In healthy mucus, mucins are connected by disulfide bonds to form a lightly crosslinked gel. In muco-obstructive lung diseases such as cystic fibrosis and asthma associated with chronic airway inflammation, immune cells, such as neutrophils and eosinophils, secrete peroxidases that catalyze the formation of reactive oxygen species.^{4–6} These reactive oxygen species can react with free cysteines to form additional disulfide crosslinks between mucins, resulting in more solid-like and stiff mucus that resists

flow. In muco-obstructive lung diseases such as asthma and cystic fibrosis, pathologic mucus builds up and blocks the airway.^{5,7,8}

Reducing agents that break down disulfide bonds between mucins can be used to treat stiffened, pathologic mucus and restore healthy mucus flow properties.^{9–11} The only FDA-approved reducing agent for this purpose is *N*-acetylcysteine; however, its clinical efficacy has been found to be limited due to low activity and a side-effect of bronchoconstriction.^{9,12} Novel reducing agents that are well-tolerated by patients with muco-obstructive lung diseases and effective at breaking down mucin crosslinks are in the process of being developed.^{4,9,13} Improved understanding of reducing agents' effect on mucus material properties is needed to aid in the design of such drugs.

Mucus-inspired hydrogels that capture aspects of the dynamic mucin network can help to elucidate the mechanisms of mucus rheology regulation in health and disease.^{14,15} We have previously demonstrated a magnetic microwire rheometer (MMWR) to measure the changes in material properties of dynamic hydrogels in response to agents that modulate disulfide-crosslinking.¹⁶ This rheological technique is nondestructive, permitting time evolution measurements of the sample rheology with minimal disturbance. In this work, we use the MMWR to compare multiple reducing agents and characterize the degradation of disulfide-crosslinked hyaluronic acid hydrogels as these agents diffuse through the network. While these reducing agents have been investigated *via* macrorheology

^a Department of Chemical Engineering, Stanford University, Stanford, CA, USA.
E-mail: ggf@stanford.edu

^b Institute of Chemistry and Biochemistry, Freie Universität Berlin, Berlin, Germany.
E-mail: haag@zedat.fu-berlin.de

^c Department of Mechanical Engineering, Stanford University, Stanford, CA, USA

^d Department of Pediatric Respiratory Medicine, Immunology and Critical Care Medicine, Charité – Universitätsmedizin Berlin, Berlin, Germany

^e German Center for Lung Research (DZL), associated partner site, Berlin, Germany

^f German Center for Child and Adolescent Health (DZKJ), partner site Berlin, Berlin, Germany

† Electronic supplementary information (ESI) available. See DOI: <https://doi.org/10.1039/d4sm01118j>

methods, we show that the diffusion of these reagents, rather than mixing, into the hydrogel reveals key differences in degradation mechanism that have major implications for drug-delivery and efficacy *in vivo*.

Materials and methods

Reducing agent preparation

Thiolated dendritic polyglycerol sulfate (dPGS-SH) was synthesized by the Haag group in Berlin following the protocol previously described.¹⁷ *N*-Acetylcysteine (NAC) and dithiothreitol (DTT) were purchased from Sigma Aldrich and Bio-Rad, respectively. 50 mM solutions of each reducing agent were prepared in 1X phosphate buffered pH 7.4 (PBS, Life Technologies) solution on the day of the experiment.

Disulfide-crosslinked hyaluronic acid hydrogel

A thiolated hyaluronic acid (HA) hydrogel was used as a mucus-mimetic material to model the disulfide-crosslinking of cysteine-rich mucin polymers. 0.25% (w/v) and 0.5% (w/v) solutions of thiolated HA (Glycosil, Advanced Biomatrix) in PBS were prepared with 10% (v/v) dimethyl sulfoxide (DMSO, Fisher Scientific) to initiate crosslinking of the disulfide bonds *via* thiol oxidation. 200 µL aliquots of the thiolated HA solution were prepared in 12 mm diameter dishes, covered and parafilm-wrapped to prevent evaporation, and allowed to cross-link into gels over 24 hours.

Magnetic microwire rheology

A magnetic microwire rheometer (MMWR) was used to measure the rheology of the hydrogels over time during degradation. The components and calibration of the device have been described previously.¹⁶ Briefly, the device consists of a magnetic microwire probe (diameter: 30 µm, length: 5 mm) that is deposited on the surface of the sample. Electromagnetic coils were used to produce a magnetic force on the microwire that caused it to translate along its longitudinal axis. The device was placed on an inverted microscope (Nikon Ti2 Eclipse, Nikon) within a standard well-plate insert, and the microwire motion was imaged with a 10× air objective. The development of the MMWR was previously described in detail and demonstrated on the same thiolated HA gels during gelation *via* an oxidizing agent, 10% (v/v) DMSO, and degradation by a reducing agent, 1 mM DTT, showing this device can make nondestructive measurements of dynamic hydrogel rheology over time and in response to various stimuli.¹⁶ Here, the same device was used to characterize the evolution of disulfide-crosslinked HA hydrogel rheology after treatment with various reducing agents *via* creep compliance measurements.

To make the creep compliance measurements, a constant magnetic force was applied to the microwire for 10 seconds, followed by an 'off' period of 20 seconds to allow the sample to relax. This procedure was repeated twice over the course of one minute, and the images of the microwire position were acquired at a rate of 2 frames per second over the course of

that minute. A custom MATLAB script was used to analyze the images and determine the microwire displacement over time. The microwire displacement relative to the magnitude of the applied force was used to calculate the compliance as a function of time. A geometric resistance factor for a cylinder translating along its longitudinal axis was used to account for the stress applied to the sample from the applied force on the microwire.¹⁸ While the microwire was placed at the surface of the sample, the interfacial contributions to the measurement were considered negligible. As discussed in detail in our previous work, the Boussinesq number, or the ratio of interfacial rheology to bulk rheology, of the samples was expected to be very small due to the viscoelasticity of the bulk material.¹⁶ Further, the compliances and viscosities measured by the MMWR were confirmed to be comparable to the quantities measured using a commercial macrorheometer.¹⁶

The compliance *versus* time data was fit with the viscoelastic Burgers model to calculate the steady-state compliance and zero-shear viscosity of the material, or the softness and resistance to flow, respectively.^{16,19} In the limit of linear viscoelasticity, when the relationship between the applied stress and the measured strain is constant, the creep compliance measurement in time is directly related to the dynamic moduli in frequency through well-known integral transformations. The steady-state compliance is then the inverse of the elastic modulus at the low shear rate limit.

At time zero, creep compliance measurements of the fully cured gels were performed in triplicate for each sample. Once the reducing agent was applied to the surface of the gel, time point measurements were made every ~2 minutes until $t = 10$ min, then every ~5–10 minutes over the course of 1 hour, and finally every 30 minutes until $t = 120$ min. A final timepoint measurement was made at $t = 24$ h. All measurements were made at room temperature of 25 °C.

Theoretical pore size calculation

A theoretical pore size of the disulfide-crosslinked HA gels was calculated using the following formula: $\xi = \left(\frac{k_B \cdot T}{G'} \right)^{\frac{1}{3}}$, where k_B is the Boltzmann constant, T is the temperature in Kelvin, and G' is the elastic modulus, which was approximated by the inverse of the steady-state compliance.²⁰

Degradation assays

To initiate degradation of the disulfide-crosslinked HA gel, 10% (v/v) of the 50 mM reducing agent solution was pipetted directly on the surface of the gel, resulting in a final concentration of 5 mM reducing agent. The reducing agent was allowed to diffuse into the gel and no mixing occurred. The MMWR was used to make creep compliance measurements and quantify the evolving rheology of the gel over time as the reducing agent degraded the sample.

Gel height measurements

The position of the microwire on the surface of the gel relative to the surface of the dish was used to measure the height of the gel. The z -position of the objective was adjusted to focus on the microwire, and that recorded z -position was extracted from the image metadata to track the wire z -position over time.

Kinetic constant determination

The rheological data of the steady-state compliance and the zero-shear viscosity *vs.* time was used to calculate an effective rate constant of the degradation reaction by fitting the data with a first order rate law, $y = y_0 \exp(-kt)$. Similarly, the gel height *vs.* time data was also fit with a first order rate law, $y = y_f - (y_f - y_0) \exp(-kt)$.

Diffusion measurements

Diffusion into 0.25% gels was examined with 20 kDa Fluorescein isothiocyanate (FITC)-dextran (Sigma Aldrich). 10% (v/v) FITC-dextran solution (0.1 mg mL⁻¹ in PBS) was pipetted onto the surface of the gel. The diffusion progress in the z -direction (downward from the surface of the gel) was captured *via* z -stack images with a spinning disk confocal microscope (Nikon Crest V3, Nikon) using a 40 \times air objective and brightfield and 488 nm channels. The images were analyzed in ImageJ by generating plots of the fluorescence intensity *vs.* z -position across time points. The data were normalized by the peak fluorescent intensity just after the FITC-dextran solution was added and by subtracting off the minimum intensity from the area outside the gel.

Results

Thiolated HA hydrogels were prepared and allowed to crosslink with 10% (v/v) DMSO for 24 hours prior to the experiments. After this time period, time zero measurements were made of

the crosslinked hydrogel rheology with the MMWR prior to addition of a reducing agent. As seen previously,¹⁶ the cured gels showed characteristics of a viscoelastic solid, with a steady-state compliance that was inversely proportional to the cross-link density of the gel, and a high zero-shear viscosity, such that little to no flow was observed. Two different gel concentrations, 0.25% (w/v) and 0.5% (w/v), were examined to investigate the role of crosslinking density on the extent of the reducing agents' effect on gel rheology. As expected, the 0.25% gel was found to have a higher compliance (increased softness) compared to the 0.5% gel, indicating a lower density of disulfide bond crosslinks in the 0.25% gel and increased pore size of the gel (Fig. 1). We calculated theoretical pore sizes based on the elasticity of the gels of ~ 80 nm for the 0.25% gel and ~ 35 nm for the 0.5% gel. These results fall within the range of viscoelastic behavior and pore sizes observed in sputum from CF patients.²¹ Gel behavior was also shown by tilting the sample and observing no flow (Fig. S1A, ESI[†]).

Gel phase rheology

After the time zero measurements, 10% (v/v) of the reducing agent solution was pipetted onto the surface of the gel, to a final concentration of 5 mM reducing agent. No mixing occurred, and the solution was allowed to diffuse into the gel. Using the MMWR, we measured the rheology of the sample over time as the reducing agents diffused into the gel. We found that the DTT-treated gels degraded rapidly, as we have seen in prior work,¹⁶ with the compliance increasing and the viscosity decreasing by orders of magnitude over the course of ~ 1.5 h (Fig. 2A). Using the steady-state compliance and zero-shear viscosity *vs.* time data from the DTT-treated gels, we fit a simple first order rate kinetics model to find an effective reaction rate constant. From both the compliance and viscosity data across trials with both the 0.25% and 0.5% gel, we found a consistent degradation rate constant of $1.6 \times 10^{-3} \pm 3 \times 10^{-4}$ s⁻¹, expressed here as the mean \pm standard deviation (Fig. 2B). In

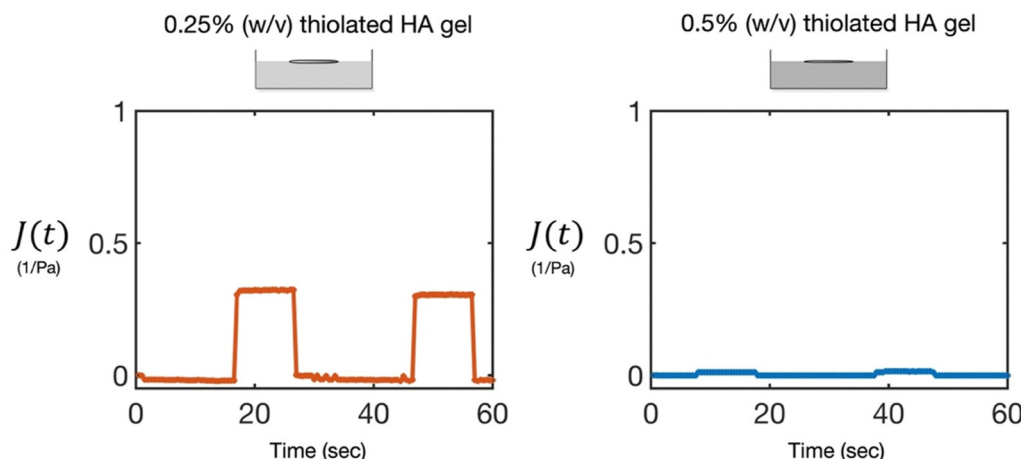


Fig. 1 Disulfide-crosslinked HA gels are viscoelastic solids of varying stiffness that depends on crosslink density. Representative creep compliance curves of the 0.25% (orange, left) and 0.5% (blue, right) disulfide-crosslinked HA gels, with schematics above demonstrating the microwire position in the samples. Both the 0.25% and 0.5% gels displayed viscoelastic solid behavior after crosslinked with DMSO for 24 h. The 0.25% had a higher compliance, indicating a softer material with a lower crosslink density. The 0.5% was stiffer with a lower compliance.

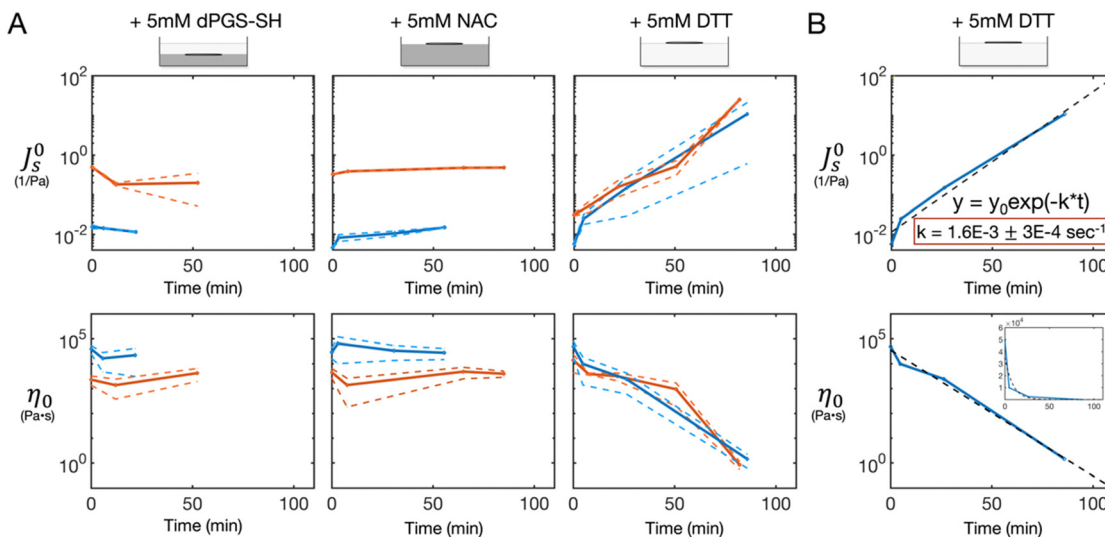


Fig. 2 Gel phase properties remain constant with dPGS-SH and NAC treatment while DTT degrades the entire gel. (A) Steady-state compliance (top) and zero-shear viscosity (bottom) of 0.25 wt% (orange) and 0.5 wt% (blue) gels as a function of time after treatment with 5 mM dPGS-SH, NAC, or DTT. The solid markers show the mean values, and the dashed lines indicate one standard deviation from the mean across 3 measurements. (B) Representative fit (dashed) of the steady-state compliance (top) and zero-shear viscosity (bottom) vs. time data (solid) of the DTT-treated gels with a first-order reaction rate model. Inset shows the same data plotted on a linear scale.

contrast, the measurements of the dPGS-SH and NAC treated gels remained consistent over the course of ~ 1 h + (Fig. 2A).

Gel height

The microscope was used to focus on the microwire probe that was located on the surface of the sample at time zero. When dPGS-SH was added to the gel surface, the microwire began to drift out of focus away from the initial gel surface and downward into the sample. During this time, the microwire measurements of the gel properties remained consistent, as noted above (Fig. 2A). After ~ 50 minutes, the microwire position reached a steady state. When the sample was picked up and tilted to check for a gel, a layer of liquid-like material was observed at the surface (Fig. S1B, ESI†), while the remainder of the sample was solid and gel-like. It appeared that the dPGS-SH had degraded the surface of the sample, leaving the remainder of the gel unaffected. The microwire height data was normalized by the height at time zero and plotted as a function of time

as a measure of the gel phase height over the course of the degradation (Fig. 3A).

For the dPGS-SH-treated gels, the gel phase height decreased rapidly, and then leveled out to a steady-state after ~ 50 min. We then fit this data with a first order rate kinetics model and found a consistent measure of the degradation rate constant across all dPGS-SH treated samples of $2.3 \times 10^{-3} \pm 3 \times 10^{-5} \text{ s}^{-1}$ (Fig. 3B). In contrast, when NAC and DTT were added to the gel, the microwire probe height remained more consistent in the case of 0.5% gel. For the 0.25% gel, some increase in the wire height was observed after the addition of NAC and DTT, which then leveled out back around the initial starting height over the course of 1.5 h. This increase in gel height was likely due to swelling of the gel with the addition of the reducing agent solution.

Rheology of degraded gel

As noted above, the initial MMWR measurements of the dPGS-SH treated gels followed the gel phase of the sample, resulting

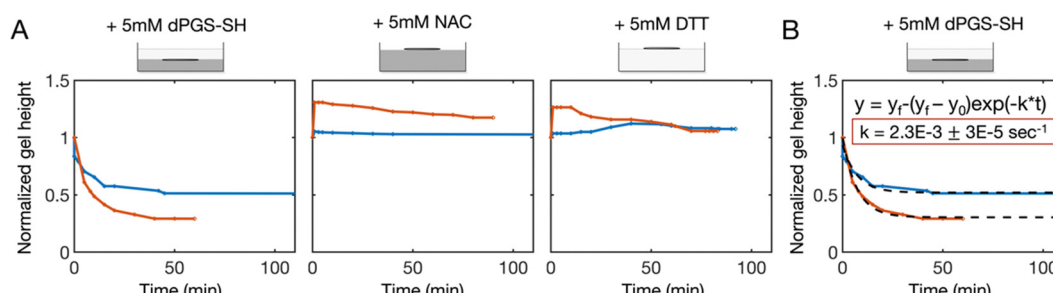


Fig. 3 Gel height decreases rapidly with dPGS-SH treatment, while it remains constant with NAC and DTT treatment. (A) Normalized gel height of the 0.25% (orange) and 0.5% (blue) gels as a function of time after treatment with 5 mM dPGS-SH, NAC, or DTT. (B) Representative fit (dashed) of the normalized gel height vs. time data (solid) of the dPGS-SH-treated gels with a first-order reaction rate model.

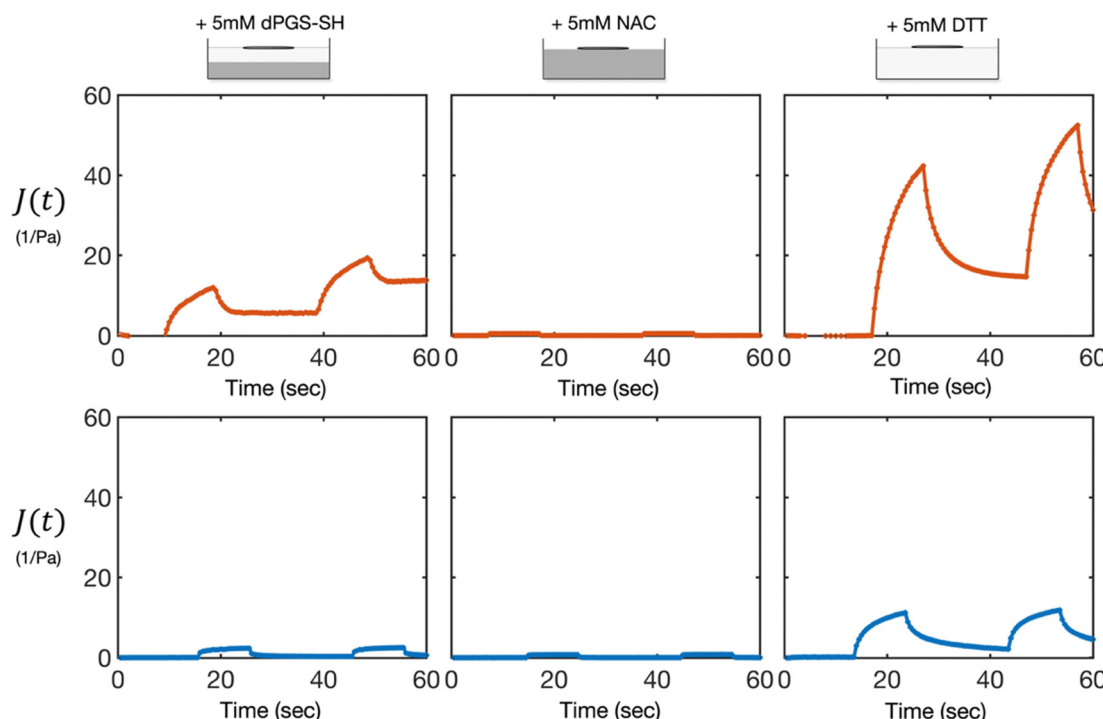


Fig. 4 dPGS-SH breaks down the gel surface, whereas DTT degrades the bulk gel into a viscoelastic liquid. Representative creep compliance curves at the surface of 0.25% (orange, top) and 0.5% (blue, bottom) HA gels at $t = 1$ h after treatment with 5 mM dPGS-SH, NAC, or DTT. dPGS-SH treated gels showed viscoelastic liquid behavior at the surface, with a higher compliance and lower viscosity than the gelled material below (shown in Fig. 2A). In contrast, the NAC-treated sample showed no change from the initial viscoelastic solid gel, and the DTT-treated samples displayed a uniform bulk viscoelastic liquid behavior, with a higher compliance and lower viscosity than the degraded dPGS-SH-treated sample.

in a measurement of viscoelastic solid properties that was consistent with the time zero measurements. When we saw that dPGS-SH had degraded the surface of the gel, resulting in a fluid layer at the surface, we retrieved the microwire from the surface of the gel and placed it instead on the surface of the liquid-like layer on top. The liquid-like layer was found to be a viscoelastic liquid (Fig. 4), indicating that dPGS-SH had reacted with the surface of the gel to break down the disulfide crosslinks, but had not penetrated deeper into the sample, leaving the crosslinked gel layer below intact. To assess whether dPGS-SH can diffuse into the gel, we conducted diffusion experiments with an inert reagent of the same molecular weight: 20 kDa FITC-dextran. We found that the FITC-dextran diffused into the 0.25% gel over the course of 40 minutes, indicating that dPGS-SH is small enough to diffuse into the gel (Fig. S2, ESI[†]).

In contrast, the NAC and DTT-treated samples showed only one phase behavior, rather than the two partitioned phases found in the dPGS-SH treated gels. The NAC-treated samples remained unchanged, displaying properties of a viscoelastic solid that were consistent with the initial time zero measurement (Fig. 4 and Fig. S1C, ESI[†]). The DTT-treated sample became a viscoelastic liquid (Fig. 4), with the entire sample flowing when tilted (Fig. S1D, ESI[†]). There was no gel-phase behavior remaining, and the samples had a higher compliance and lower viscosity than the liquid-phase of the dPGS-SH-treated gels, indicating a higher number of crosslinks were broken down, resulting in a softer and more flowable material.

Long-time behavior of degraded gel

24 hours after the initial addition of the reducing agents, we returned to the treated samples to determine if any further changes had occurred beyond $t = 2$ h. We found the dPGS-SH treated sample unchanged, with a degraded, liquid-like phase at the surface, and a crosslinked gel phase below. In contrast, the once liquid-like DTT-treated sample had returned to a crosslinked gel. Creep compliance measurements were repeated at $t = 24$ h to confirm this assessment (Fig. 5).

Discussion

In this work, we used the MMWR to characterize the degradation of a mucus-mimetic thiolated HA hydrogel by disulfide reducing agents. Prior work by others has employed macro-rheology, such as a cone and plate rheometer, to measure the material response of patient sputum to degradation by disulfide reducing agents.^{4,9,13,17} While this is an effective method to gain a general understanding of the effect of a reducing agent on the gel material properties, this experimental technique requires spreading the initial gel onto the rheometer with a spatula or pipette and then mixing the reducing agent into the sample to measure a uniform, homogeneous response. This procedure likely obscures key factors of the degradation process that would be relevant *in vivo* such as how the reagent reacts as it diffuses through the gel. With the MMWR, we

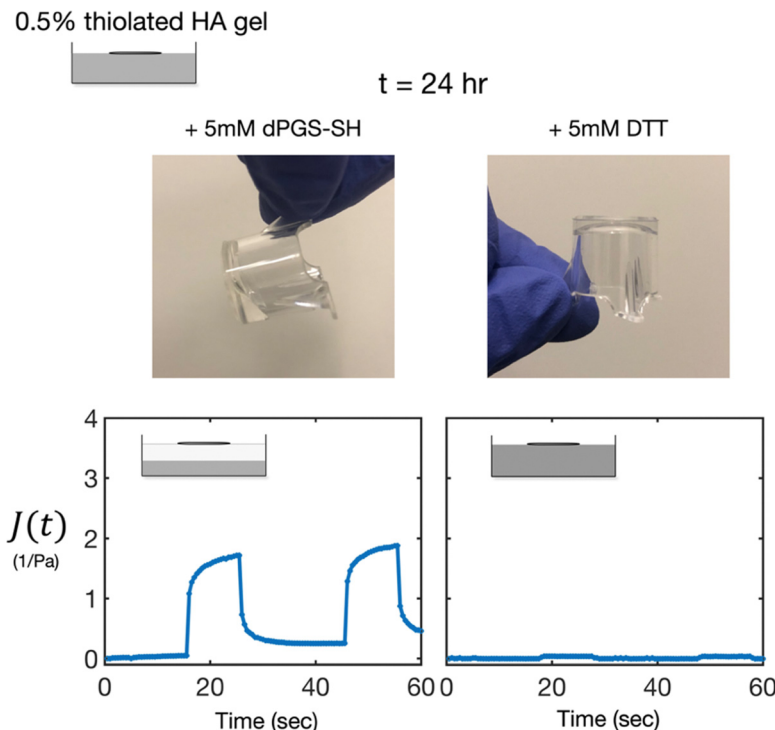


Fig. 5 dPGS-SH treated samples retain a viscoelastic liquid layer 24 hours after initial treatment, whereas DTT treated samples return to a crosslinked gel. Representative images (top) and creep compliance curves (bottom) at the surface of 0.5% HA gels at $t = 24$ h after treatment with 5 mM dPGS-SH (left) or DTT (right). dPGS-SH treated gels continued to show a viscoelastic liquid layer at the surface, with a gel phase below, as seen previously at $t = 1$ h. In contrast, the DTT-treated samples returned to a crosslinked gel, displaying viscoelastic solid properties similar to the time zero behavior.

minimize disturbance to the gel structure during rheological characterization and track the rheology of the sample as the reducing agent diffuses into the gel, giving us insight into the mechanism of degradation.

The three disulfide reducing agents examined in this work, dPGS-SH, DTT, and NAC, were compared on an equimolar basis of 5 mM. Previous work examined the mucolytic effect of varying concentrations of these reducing agents on the mucin size of sputum.¹⁷ That work showed that both dPGS-SH and DTT, but not NAC, had potent mucolytic activity at 5 mM. Further, NAC is the only clinically approved reducing agent for use in patients. The concentration used in this study is in the range of concentrations that can be achieved *via* inhalation therapy in patients, thus providing a clinically meaningful reference for this work.¹³

With our MMWR measurements of the degradation of disulfide-crosslinked HA hydrogel by reducing agents, we find evidence that addition of dPGS-SH surface erodes the gel, while DTT acts *via* bulk degradation. dPGS-SH degraded the surface of the gel, resulting in a viscoelastic liquid at the surface and leaving the remainder of the sample unchanged. In contrast, the entire DTT-treated sample became softer and more flowable over time, as crosslinks throughout the entire sample were broken down. This difference in mechanism likely arises from variations in the ratio of the reaction rate to diffusion rate between these two reagents and the disulfide-crosslinked HA hydrogel.²²

By fitting the degradation data with a first order reaction rate law, we were able to measure effective rate constants for both dPGS-SH and DTT, and we found the rate constant for dPGS-SH to be only $\sim 1.5 \times$ faster than that of DTT. This result agrees with prior work that has found a similar activity between these reagents.¹⁷ However, notably, these two molecules differ in size. dPGS-SH is the larger of the two reagents (20 kDa). The chemical structures and molecular weights of the reducing agents are shown in Fig. S3A and B (ESI[†]). Previous measures of the hydrodynamic radius of dPGS-SH have reported values of ~ 6 nm,¹⁷ which falls below the theoretical pore sizes calculated for these gels (35 and 80 nm), indicating that dPGS-SH is small enough to diffuse into the gel. Additionally, the diffusion capability of dPGS-SH has been previously demonstrated in patient sputum with an approximate pore size of 70 nm *via* FRAP measurements.¹⁷ Further, in this work we showed that an inert polymer of the same molecular weight, 20 kDa FITC-dextran, diffuses throughout the 0.25% gel in ~ 40 minutes (Fig. S2, ESI[†]). However, the theoretical time scale of this diffusion process will be affected by molecule size. DTT is a much smaller molecule (154 Da), approximately 100 \times smaller than dPGS-SH, and as a result, it can diffuse $\sim 100 \times$ faster. dPGS-SH reacts faster than it diffuses into the gel, resulting in a surface erosion of the gel where the bottom layer of the sample remains fully gelled, and the top layer is broken down into a viscoelastic liquid. In contrast, DTT diffuses faster than it reacts, leading to a bulk degradation of the gel which results

in the entire sample becoming a viscoelastic liquid. Finally, we find that NAC is not effective at 5 mM concentration in both the 0.25% and 5% gels, and we observed no significant change in gel properties with this treatment. This result agrees with previous work by others that has found NAC has low activity and little effect in increasing the fluidity of airway mucus.^{9,13} While these reducing agents have varying degrees of thiolation (Fig. S3, ESI†), these conclusions regarding bulk reduction, surface erosion, and kinetics are independent of the molar amounts of the thiol groups present. Further, the reducing effect is not solely dependent on the number of thiol groups applied. Parameters such as thiol acidity and reduction potential have a decisive influence. Moreover, previous work has observed that DTT is more potent than both NAC and dPGS-SH to reduce disulfide bonds as shown in western blot analysis of treated sputum.¹⁷

Of note, while the degradation reaction finished within ~ 2 hours, when we returned to the samples 24 hours later, the DTT-treated gels had returned to their initial state of a solid-like gel. In contrast, the dPGS-SH-treated samples retained the same volume ratio of liquid and gel layers, and the liquid layer remained flowable. This difference in long-time fate of the degraded gel likely occurs due to the monothiol *versus* dithiol nature of these reagents. When dPGS-SH, a polymer possessing multiple monothiols, reduces a disulfide bond, it results in capped thiol. In the case of DTT, a dithiol, two reduction reactions occur in succession, resulting in two free thiols that can re-oxidize. In our case, the DTT-treated samples likely re-oxidized due to exposure to oxygen in the air. This is an important observation for clinical development, as an effective mucolytic is desired to have a sustained effect on the treated mucus.

In conclusion, we found differences in both the mechanism of degradation and the long-time fate of disulfide-crosslinked hydrogels treated with various reducing agents. With our MMWR device, we made creep compliance measurements of the degrading hydrogels to assess how material rheology evolved over time during degradation with dPGS-SH, NAC, and DTT. With this nondestructive technique, we were able to assess the mechanism of degradation, as the reducing agent was allowed to diffuse through the sample in the absence of forced mixing. While the activity of dPGS-SH and DTT was found to be similar, the much larger size, and thus slower diffusion, of dPGS-SH results in a difference in degradation mechanism: dPGS-SH surface erodes the gel, whereas DTT diffuses much faster and bulk degrades the sample. This difference in degradation mechanism based on the relationship between the diffusion rate and the reaction rate of the reducing agent in the gel could be tuned to optimize the desired clinical outcome and maintain a layer of protective mucus on the epithelial cell surface. Additionally, the dithiol-nature of DTT resulted in a re-oxidation and re-gelation of the sample 24 hours after the initial treatment. Both the degradation mechanism and long-time fate are critical considerations when designing new reducing agent drugs for treatment of muco-obstructive diseases.

Data availability

The data that support the findings of this study are available from the corresponding author upon request.

Conflicts of interest

The authors have no conflicts of interests to disclose.

Acknowledgements

M. B. acknowledges support from the National Science Foundation Graduate Research Fellowship (NSF GRFP) and the Cystic Fibrosis Trust. R. H. and M. A. M. are funded by the Deutsche Forschungsgemeinschaft (DFG, German Research Foundation) – Project ID 431232613 – SFB 1449 (Project B03, Project C04). The authors acknowledge Professor Manuel Vazquez Villalabeitia at the Institute of Material Science of Madrid, Spanish National Research Council (CSIC) for providing magnetic microwires.

References

- 1 C. E. Wagner, K. M. Wheeler and K. Ribbeck, Mucins and Their Role in Shaping the Functions of Mucus Barriers, *Annu. Rev. Cell Dev. Biol.*, 2018, **34**, 189–215.
- 2 P. Verdugo, Supramolecular dynamics of mucus, *Cold Spring Harbor Perspect. Med.*, 2012, **2**(11), a009597.
- 3 B. Demouveau, V. Gouyer, F. Gottrand, T. Narita and J. L. Desseyn, Gel-forming mucin interactome drives mucus viscoelasticity, *Adv. Colloid Interface Sci.*, 2018, **252**, 69–82.
- 4 S. Yuan, M. Hollinger, M. E. Lachowicz-scroggins, S. C. Kerr, E. M. Dunican and B. M. Daniel, *et al.*, Oxidation increases mucin polymer cross-links to stiffen airway mucus gels, *Sci. Transl. Med.*, 2015, **7**(276), 276ra27.
- 5 E. M. Dunican, B. M. Elicker, D. S. Gierada, S. K. Nagle, M. L. Schiebler and J. D. Newell, *et al.*, Mucus plugs in patients with asthma linked to eosinophilia and airflow obstruction, *J. Clin. Invest.*, 2018, **128**(3), 997–1009.
- 6 S. Y. Graeber and M. A. Mall, The future of cystic fibrosis treatment: from disease mechanisms to novel therapeutic approaches, *Lancet.*, 2023, **402**(10408), 1185–1198.
- 7 L. M. Kuyper, P. D. Paré, J. C. Hogg, R. K. Lambert, D. Ionescu and R. Woods, *et al.*, Characterization of airway plugging in fatal asthma, *Am. J. Med.*, 2003, **115**(1), 6–11.
- 8 M. A. Mall, P. R. Burge, C. Castellani, J. C. Davies, M. Salathe and J. L. Taylor-Cousar, Cystic fibrosis, *Nat. Rev. Dis. Primers.*, 2024, **10**(53), 1–26.
- 9 C. Ehre, Z. L. Rushton, B. Wang, L. N. Hothem, C. B. Morrison and N. C. Fontana, *et al.*, An improved inhaled mucolytic to treat airway muco-obstructive diseases, *Am. J. Respir. Crit. Care Med.*, 2019, **199**(2), 171–180.
- 10 L. E. Morgan, A. M. Jaramillo, S. K. Shenoy, D. Raclawska, N. A. Emezienna and V. L. Richardson, *et al.*, Disulfide disruption reverses mucus dysfunction in allergic airway disease, *Nat. Commun.*, 2021, **12**(1), 249.

11 M. A. Liegeois, M. Braunreuther, A. R. Charbit, W. W. Raymond, M. Tang and P. G. Woodruff, *et al.*, Peroxidase-mediated mucin cross-linking drives pathologic mucus gel formation in IL-13-stimulated airway epithelial cells, *JCI Insight*, 2024, **9**(15), e181024.

12 R. M. Marrades, J. Roca, J. Albert Barberà, L. de JOVER, W. M. Ac Nee and R. Rodriguez-roisin, Nebulized Glutathione Induces Bronchoconstriction in Patients with Mild Asthma, *Am. J. Respir. Crit. Care Med.*, 1997, **156**, 425–430.

13 A. Addante, W. Raymond, I. Gitlin, A. Charbit, X. Orain and A. W. Scheffler, *et al.*, A novel thiol-saccharide mucolytic for the treatment of muco-obstructive lung diseases, *Eur. Respir. J.*, 2023, **61**(5), 2202022.

14 A. Sharma, B. Thongrom, S. Bhatia, B. von Lospichl, A. Addante and S. Y. Graeber, *et al.*, Polyglycerol-Based Mucus-Inspired Hydrogels, *Macromol. Rapid Commun.*, 2021, **42**(20), 2100303.

15 R. Bej and R. Haag, Mucus-Inspired Dynamic Hydrogels: Synthesis and Future Perspectives, *J. Am. Chem. Soc.*, 2022, **144**, 20137–20152.

16 M. Braunreuther, M. Liegeois, J. V. Fahy and G. G. Fuller, Nondestructive rheological measurements of biomaterials with a magnetic microwire rheometer, *J. Rheol.*, 2023, **67**(2), 579–588.

17 J. Arenhoevel, A. Kuppe, A. Addante, L. F. Wei, N. Boback and C. Butnarasu, *et al.*, Thiolated polyglycerol sulfate as potential mucolytic for muco-obstructive lung diseases, *Biomater. Sci.*, 2024, **12**, 4376–4385.

18 M. M. Tirado, J. Garda and D. Torre, Translational friction coefficients of rigid, symmetric top macromolecules. Application to circular cylinders, *J. Chem. Phys.*, 1979, **71**(6), 2581–2587.

19 K. Te Nijenhuis, G. H. McKinley, S. Spiegelberg, H. A. Barnes, N. Askel and L. Heymann, *et al.*, in *Non-Newtonian Flows*, ed. C. Tropea, A. Yarin, J. F. Foss, *Springer Handbook of Experimental Fluid Mechanics*, Springer, 2007, pp. 619–744.

20 P. J. Flory and J. Rehner, Statistical mechanics of cross-linked polymer networks I. Rubberlike elasticity, *J. Chem. Phys.*, 1943, 512–520.

21 L. Schaupp, A. Addante, M. Völler, K. Fentker, A. Kuppe and M. Bardua, *et al.*, Longitudinal effects of elexacaftor/tezacaftor/ivacaftor on sputum viscoelastic properties, airway infection and inflammation in patients with cystic fibrosis, *Eur. Respir. J.*, 2023, **62**(2), 2202153.

22 F. Von Burkersroda, L. Schedl and A. G. Opferich, Why degradable polymers undergo surface erosion or bulk erosion, *Biomaterials*, 2002, **23**, 4221–4231.